A Preliminary Study on UAV Thermal Sensing for Geothermal Prospecting

Jin-King LIU [1], Wei-Chen HSU [2] and En-Kai LIN [3]

[1]CEO, LIDAR Technology Co., Ltd., Hsinchu County 30274, Taiwan. jkliu@lidar.com.tw

[2]General Manager, LIDAR Technology Co., Ltd., Hsinchu County 30274, Taiwan. ianhsu@lidar.org.tw

[3]Project Manager, LIDAR Technology Co., Ltd., Hsinchu County 30274, Taiwan. easyko23@lidar.com.tw

Abstract: Traditional airborne hyperspectral thermal images were obtained by an integrated system combining an additional airborne LiDAR and the thermal infrared sensor. The results of thermal imaging by a UAV Sensor were evaluated to understand the potential in geothermal prospecting, The geometric accuracy for both sensor systems is comparable whereas the radiometric issue for the low grade sensor onboard a drone remains to be improved before it can be effectively applied for quantitative assessment of geothermal reserves.

Keywords: remote sensing, airborne LiDAR, hyperspectral, geothermal prospecting

1. Introduction

Geothermal systems are increasingly important as sources of renewable energy in Taiwan due to the high thermal gradients observed in this tectonic collision place on the earth surface. Thermal infrared (TIR) remote sensing provides a unique tool for mapping the surface expressions of geothermal activity. Airborne high-resolution thermal infrared (TIR) remote sensing has proven to be an effective method for mapping surface spatial temperature patterns (Chen et al., 2015; Liu et al., 2015; Jao et al., 2015; Liu et al., 2015). As geothermal energy continues to be a source of safe, reliable and renewable source of energy, TIR remote sensing becomes a key component of geothermal exploration. When combined with other spatial datasets, the TIR data showed areas of thermal influence resulting from geothermal activity associated with point, area and linear sources such as fumaroles, hot ground, fissures and faults (Phillips et al., 2013; Garner and Budd, 2015; Meer et al., 2014). Nevertheless, the cost for aerial survey can be substantially reduced if a UAV platform (a drone) can be used to substitute an airplane. The load carrying capacity and range of a drone set a strict limitation. Thus, only very light and low grade thermal sensor can be employed. It is worthwhile to explore the feasibility of replacing traditional airborne thermal sensing with a drone system.

The purpose of this study is to compare the results of thermal imaging by a ThermoMAP Drone Sensor onboard eBee and an airborne thermal imager SPECIM AisaOWL onboard an integrated system combining an additional airborne LiDAR and the thermal infrared sensor.

2. Airborne Thermal Sensing

An integrated system combining an airborne LiDAR and a thermal infrared sensor was established and tested in this study for obtaining high accuracy thermal images of the ground surface of the Tatun Volcanic Area. Due to the high accuracy of POS (Positioning and Orientation System) of the integrated system, the positioning accuracy is higher than 15 cm. With airborne LiDAR, DTM (Digital Terrain Models) of 1 m grid and 50 cm height accuracy are achieved. The utmost important is the

temperature accuracy of the thermal sensor is 0.1 degree centigrade. In addition, an amalgamated effected was achieved to combine the 3D coordinates of laser points with the fourth dimension of temperature of each individual points.

An AisaOWL Airborne Hyperspectral Imaging System was used in the study. The AisaOWL sensor covers full LWIR 7.7 to 12.3 μm with 96 spectral bands. The swath is with 384 pixels and with an FOV (Field of View) of 32 degrees. With a flight height above average ground level of 1400 m of the experiment, the spatial resolution of thermal images and digital terrain models are resampled to 1 m grid.

. Ground observations of dynamic temperatures at selected sites are also carried out for obtaining temperature variations of the sites for verification purpose and thus to understand diurnal heating effects of the ground. This is important to understand the effectiveness to relate radiant temperatures by thermal imager and kinematic temperature of the ground. In addition, this is also important to quantify the effect of emissivity for the radiant temperatures.

Two major results of this newly-designed integrated system were achieved in this experiment. One is the technique for obtaining accurate surface temperature of a large area, that is accurate ground surface temperature mapping. The other is that heat flow or heat discharge rate of the thermal anomaly areas can be assessed with the airborne temperature map.

3. UAS Thermal Imaging

Aerial surveying through the ThermoMAP Drone Sensor onboard an eBee drone allows the drone camera to capture thermal drone video and still images for creating a full thermal map of a site. eBee drone is a product of Sensefly. SenseFly ThermoMAP (FLIR) sensor acquires images of 640x512 16bit TIFF with EXIF format. The acquired thermal images are then produced by senseFly's Postflight Terra 3D photogrammetry software (powered by Pix4D) for geometric registration to geodetic coordinates. The drone's still images were transformed into centimetre accurate 2D orthomosaics and 3D models using this type of photogrammetry software.

4. A Comparison

A common area of airborne mission and drone mission is elected for the comparison, as shown in Figure 1 and Figure 2. Figure 1 shows a mosaic of thermal image at the XiaoYokeng area of Tatun Volcanic Group acquired on 16 November 2015 by an eBee thermal imager SenseFly ThermoMAP. Figure 2 shows a mosaic of thermal image at the XiaoYokeng area of Tatun Volcanic Group acquired on 16 November 2015 by an airborne thermal imager SPECIM AisaOWL. Both geometric and radiometric properties of these two thermal images can be inspected for a comparison of the features of respective sensor systems.

As shown in Table I, the images acquired by drone give a rather high ground resolution and thus provide better geometric features.

The ThermoMap image gives a temperature range of 15.8℃to 37.2℃ whereas AisaOWL image gives a range of 17.0 ℃ to 59.2 ℃. It is obvious that a great difference of the temperature ranges of the two sensors. For further comparison of the temperature maps, the temperature ranges are classified into 8 categories as follows: (1). 0 – 10 ℃; (2) 10 – 20 ℃; (3) 20 – 25 ℃; (4) 25 – 30 ℃; (5) 30 – 35 ℃; (6) 35 – 40 ℃; (7) 40 – 50 ℃; (8) 50 – 60 ℃.

It is show in Figure 3 that (1) for most of the area, ThermoMap gives higher temperatures; whereas (2) for

the fumerales of the volcanic activities, ThermoMap gives a relatively low temperature. There is no class 7 and class 8 on ThermoMap image. Because the high temperature area of the volcanic fumaroles usually remains quite similar over the years, the low temperatures under 40 degrees acquired by drone sensor is quite abnormal. This fact shows that the temperature map acquired by ThermoMap sensor should be further calibrated for geothermal applications.

5. Conclusions

The geometric details given by drone thermal images looks superior to airborne thermal images. The drone thermal sensor gives a low temperature in volcanic volcanic fumaroles. The geometric accuracy for both sensor systems is comparable whereas the radiometric issue for the low grade sensor onboard a drone remains to be improved before it can be effectively applied for quantitative assessment of geothermal reserves. Because geothermal prospecting requires accurate temperature of the ground surface, the core issue for drone thermal imaging would be on the improvement of radiometric accuracy of the thermal sensor or to have some kind of calibration techniques.

Table I. A comparison of the drone and airborne systems

Sensor	*ThermoMAP*	*AisaOWL*
Flight height (meter) (above average sea level)	*990*	*2110*
Spectral range (μm)	*7~15*	*7.7~12.3*
Temperature sensitivity (℃)	*0.1*	*0.015*
Ground resolution (meter)	*0.15*	*2.0*

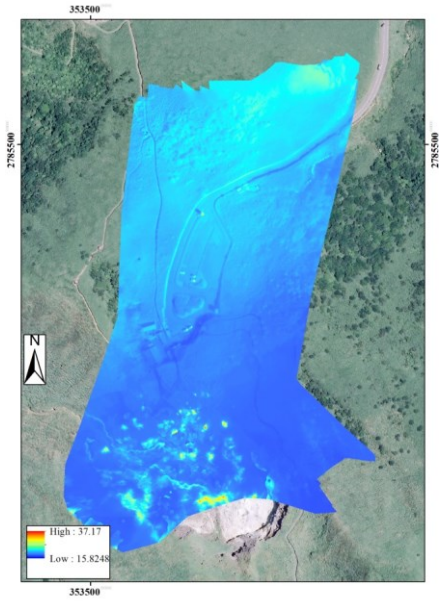

Figure 1.A mosaic of thermal image at the XiaoYokeng area of Tatun Volcanic Group acquired on 16 November 2015 by an eBee thermal imager SenseFly ThermoMAP.

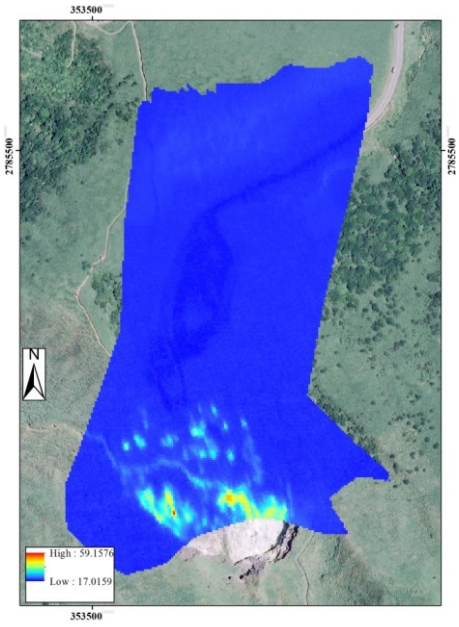

Figure 2.A mosaic of thermal image at the XiaoYokeng area of Tatun Volcanic Group acquired on 16 November 2015 by an airborne thermal imager SPECIM AisaOWL.

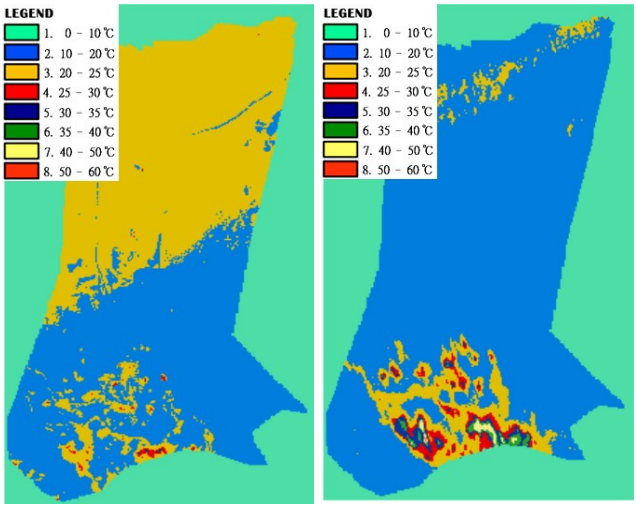

ThermoMap classified image AisaOWL classified image

Figure 3. A comparison of the 2 classified images shows that (1) for most of the area, ThermoMap gives higher temperatures; whereas (2) for the area of volcanic fumaroles, ThermoMap gives a relatively low temperature. There is no class 7 and class 8 on ThermoMap image.

References

Chih-Yu Chen, Yu-Cheng Chen, Jin-King Liu, Andreas Matzarakis, Tzu-Ping Lin, 2015 The Application of High Resolution Thermal Images Combined with Airborne LiDAR Data in Urban Thermal Environment — A Case Study in New Taipei Banqiao District. 2015 ICEO&SI and ICLEI Resilience Forum (2015 ICEO&SI and ICLEI), JUNE 28-30, Kaohsiung. Taiwan.

Fang-Ju Jao, Jin-King Liu, Wei-Chen Hsu, En-Kai Lin, and Hung-Cheng Chang, 2015. Radiometric Normalizaion of Airborne Thermal Infrared Imaging in Tatun Volcanic Group, Northern Taiwan. 2015 ICEO&SI and ICLEI Resilience Forum (2015 ICEO&SI and ICLEI), JUNE 28-30, Kaohsiung. Taiwan. PAPER No. : #ICEO-C-001P.

Gerner, E., & Budd, A. Australian Surface Temperature Corrections for Thermal Modelling. Proceedings World Geothermal Congress 2015 Melbourne, Australia, 19-25 April 2015.

Haselwimmer, C., & Prakash, A. (2013). Thermal infrared remote sensing of geothermal systems. In Thermal Infrared Remote Sensing (pp. 453-473). Springer Netherlands.

Jin-King Liu, Hung-Cheng Chang, Wei-Chen Hsu, Fang-Ju Jao, En-Kai Lin, 2015. Using Airborne Thermal Infrared Imaging to Assess the Heat Discharge Rates in Dayokeng Area, Tatun Volcanic Group, Northern Taiwan. 2015 ICEO&SI and ICLEI Resilience Forum (2015 ICEO&SI and ICLEI), JUNE 28-30, Kaohsiung. Taiwan. PAPER No. : #ICEO-C-003.

Jin-King Liu, Hung-Cheng Chang, Wei-Chen Hsu, Fang-Ju Jao, En-Kai Lin, 2015. Using Airborne Thermal Infrared Imaging to Assess the Heat Discharge Rates in Xiaoyoukeng Fumerale Area, Tatun Volcanic Group, Northern Taiwan. The International Symposium on Remote Sensing (ISRS 2015). 22-24 April, 2015. Tainan, Taiwan.

Mutua, J. (2013). High resolution airborne thermal infrared remote sensing study, Silali geothermal prospect, Kenya.

Nishar, A., Richards, S., Breen, D., Robertson, J., & Breen, B. (2016). Thermal infrared imaging of geothermal environments by UAV (Unmanned aerial vehicles). Journal of Unmanned Vehicle Systems, (ja).

Phillips, B. R., Ziagos, J., Thorsteinsson, H., & Hass, E. (2013, February). A roadmap for strategic development of geothermal exploration technologies. In Proceedings, Thirty-Eighth Workshop on Geothermal Reservoir Engineering (pp. 11-13).

van der Meer, F., Hecker, C., van Ruitenbeek, F., van der Werff, H., de Wijkerslooth, C., & Wechsler, C. (2014). Geologic remote sensing for geothermal exploration: A review. International Journal of Applied Earth Observation and Geoinformation, 33, 255-269.

Nishar, A., Richards, S., Breen, D., Robertson, J., & Breen, B. (2016). Thermal infrared imaging of geothermal environments and by an unmanned aerial vehicle (UAV): A case study of the Wairakei–Tauhara geothermal field, Taupo, New Zealand. Renewable Energy, 86, 1256-1264.